Ind. J. Pharm. Edu. Res., 2024; 58(4):1225-1234.
https://www.ijper.org

Original Article

Synthesis and Characterization of Novel Chitosan-Nickel oxide Based Amygdalin Hybrid Nanomaterials for Antibacterial and Anticancer Properties

Karunakaran Saravanan[1], Muruganantham Bharathi[2], Nouf M. Alyami[3], Sulaiman Ali Alharbi[4], Samer Hasan Hussein-Al-Ali[5], Palanisamy Arulselvan[6,*]

[1]Department of Chemical Engineering, KPR Institute of Engineering and Technology, Avinashi Road, Arasur, Coimbatore, Tamil Nadu, INDIA.
[2]Centre for Bioinformatics, Department of Biochemistry, Karpagam Academy of Higher Education, Coimbatore, Tamil Nadu, INDIA.
[3]Department of Zoology, College of Science, King Saud University, Riyadh, SAUDI ARABIA.
[4]Department of Botany and Microbiology, College of Science, King Saud University, Riyadh, SAUDI ARABIA.
[5]Department of Chemistry, Faculty of Sciences, Isra University, Amman, JORDAN.
[6]Department of Chemistry, Saveetha School of Engineering, Saveetha Institute of Medical and Technical Sciences (SIMATS), Saveetha University, Chennai, Tamil Nadu, INDIA.

ABSTRACT

Background: Nanotechnology has made tremendous progress in drug development and delivery. The functionalization of nanoparticles with various biological agents facilitates the drug delivery and treatment of various cancers. **Objectives:** The current work was conducted to synthesize the chitosan-nickel oxide-amygdalin hybrid nanomaterials (Chitosan-NiO-Amygdalin HNMs) and evaluate their antimicrobial and cytotoxic effects on liver cancer (Hep3B) and breast cancer (MCF-7) cells. **Materials and Methods:** The synthesized Chitosan-NiO-Amygdalin HNMs were characterized using various methods, including UV-visible spectroscopy, PL, XRD, DLS, SEM, TEM and FT-IR analyses. The antibacterial property of Chitosan-NiO-Amygdalin HNMs was assessed by the disc diffusion method against various pathogens. The cytotoxicity of Chitosan-NiO-Amygdalin HNMs on Hep3B and MCF-7 cells was assessed by an MTT assay. **Results:** The synthesis of Chitosan-NiO-Amygdalin HNMs was confirmed by a UV-vis spectrophotometry study. The PL emission spectrum of the Chitosan-NiO-Amygdalin HNMs shows their optoelectronic properties. The XRD patterns reveal that the HNMs possess a cubic crystal structure. The SEM images showed that the HNMs exhibit hexagonal structures. TEM images illustrate HNMs with hexagonal morphology. The HNMs have also shown potential antibacterial effects against various pathogens. The Chitosan-NiO-Amygdalin HNMs effectively inhibited the viability of both Hep3B and MCF-7 cells. **Conclusion:** The results of this work suggest that Chitosan-NiO-Amygdalin HNMs exhibit potential to be a prospective therapeutic agent in the future to treat cancer and other diseases.

Keywords: Nanomaterials, Amygdalin, Liver cancer, Drug delivery, Chitosan.

Correspondence:
Dr. Palanisamy Arulselvan
Department of Chemistry, Saveetha School of Engineering, Saveetha Institute of Medical and Technical Sciences (SIMATS), Saveetha University, Chennai, Tamil Nadu, 602 105, INDIA.
Email ID: arulbio@gmail.com

Received: 26-05-2024;
Revised: 04-06-2024;
Accepted: 22-08-2024.

INTRODUCTION

Nanotechnology is a fast-growing subject that focuses on the design, development, surface analysis, and application of materials at the nanoscale, which typically have diameters between 1 and 100 nm. Nanoscale materials or nanoparticles exhibit distinct physicochemical and biological characteristics compared to their bulk counterparts.[1] In the medical domain, nanoparticles have been employed for the purposes of drug delivery, developing novel pharmaceuticals, disease diagnosis and treatment.[2] Researchers have shown significant interest in bio-nanotechnology in recent years, as it has found widespread use in various scientific areas, particularly in the development of novel bioactive materials.[3] The basic element of drug delivery systems is the amalgamation of a suitable carrier with one or more drug components. The primary requirements for ideal delivery systems involve the localization of the active compound at the specific site of action in the body and the delivery of an accurate dosage at a consistent, appropriate and specified time.[4] Biopolymers offer significant benefits for human health and nutrition due to their exceptional properties.

Chitosan is a polysaccharide obtained from chitin through the process of deacetylation. Chitosan has received significant attention in the pharmaceutical and biomedical areas because of its advantageous characteristics.[5, 6] Nickel oxide (NiO) nanoparticles have exceptional catalytic, optical, electrical, and magnetic characteristics, which makes them suitable for various

DOI: 10.5530/ijper.58.4.135

applications. The NiO NPs possess favorable characteristics such as a substantial surface area, affordability, availability, and stability, which make them highly suitable for serving as nanoreinforcing agents in polymers and biopolymers.[7]

Breast cancer is a prevalent form of cancer in women, representing 30% of all diagnosed cancer incidences. In 2020, breast cancer was responsible for 2.3 million new incidences and 685,000 mortalities, making it the sixth most common cause of cancer-associated mortalities worldwide. The 5-year survival rate for breast cancer in all stages is 90%. Nevertheless, as the stage of cancer advances, the rate of survival reduces.[8] Liver cancer is the most prevalent type of cancer in Asia and the third-most common cause of cancer-related deaths worldwide.[9] Nanotechnology has made tremendous developments in the area of drug delivery. For example, the use of nanoparticles in the cancer treatment has progressed to the extent that it is now capable of detecting and specifically targeting an individual cancer cell by delivering a carrier to treat it. Conventional cancer treatment methods are associated with adverse effects, while diagnostic tests are costly and time-consuming. The functionalization of nanoparticles with diverse biological molecules facilitates drug delivery and the diagnosis of malignant cells.[10]

There has been a recent increase in interest in natural products because of their versatile pharmacological effects and reduced toxicity when used to develop potential drugs.[11] Amygdalin is a cyanogenic diglucoside that occurs in the seeds of several fruits and plants from the Rosaceae family. There is increasing evidence to suggest that amygdalin has anti-cancer activity against various tumor cells.[12-14] Amygdalin demonstrates a synergistic effect when amalgamated with other compounds, such as cisplatin, resulting in the induction of cell death in cancer cells.[15] Therefore, the current work was conducted to synthesize and characterize the chitosan-nickel oxide-amygdalin hybrid nanomaterials (Chitosan-NiO-Amygdalin HNMs) and evaluate their antimicrobial and cytotoxic effects on Hep3B and MCF-7 cells.

MATERIALS AND METHODS

Chemicals

Amygdalin, chitosan, nickel nitrate, Muller-Hinton agar (MHA) and other chemicals were procured from Sigma Aldrich, USA.

Synthesis of Chitosan-NiO-Amygdalin HNMs

Chitosan-NiO-Amygdalin HNMs were synthesized using the chemical precipitation process. The 0.1 M nickel nitrate and 500 mg of chitosan were dissolved with acetic acid (1%) in 50 mL of aqueous solution. Additionally, 50 mg of amygdalin was combined with a NiO-Chitosan solution. About 0.1 M of NaOH solution was mixed to the Chitosan-NiO-Amygdalin solution. A white residue has been obtained, which was vortexed for 3 h using a magnetic stirrer. The obtained residue was rinsed thrice using distilled water and an ethanol solution. The final suspension was centrifuged at 15,000 rpm, and the resultant residue was dried at 200 °C for 2 h.

Characterization of the Chitosan-NiO-Amygdalin HNMs

The UV-visible spectra of the Chitosan-NiO-Amygdalin HNMs were obtained using a JASCO770-UV-vis spectrophotometer (Tokyo, Japan). The Chitosan-NiO-Amygdalin HNMs were analyzed by photoluminescence (PL) analysis, and their spectrum was obtained using the F-2500 FL Spectrophotometer (Hitachi, Japan). The X-ray diffraction (XRD) patterns of the Chitosan-NiO-Amygdalin HNMs were acquired using an XRD-600 Diffract meter (Shimadzu, Tokyo, Japan) at 30 kV and 30 mA. The scanning rate was set at 2°/min, and the XRD measurements were taken between the 2-60° ranges of 2 Θ angles. The hydrodynamic diameter of the Chitosan-NiO-Amygdalin HNM particles was measured using a Malvern Zetasizer Nano ZS device (Malvern Instruments, UK). The scanning electron microscope (SEM; FEI, USA) was employed to study the surface morphology of Chitosan-NiO-Amygdalin HNMs. The 5 µL of sample was placed on an aluminum stub and dehydrated overnight at 37°C. An EDX spectrometer in conjunction with the SEM was utilized to investigate the elemental profile of the Chitosan-NiO-Amygdalin HNMs. The transmission electron microscopy (TEM) analysis of Chitosan-NiO-Amygdalin HNMs was conducted using a Hitachi H-7100 TEM machine. The samples were diluted using acetone and then dehydrated overnight at 37°C on 200 mesh carbon-coated TEM copper grids. The surface functional groups of Chitosan-NiO-Amygdalin HNMs were studied by Fourier transform infrared spectroscopy (FT-IR) using the Thermo Nicolet-6700 (Thermo Scientific, USA).

Antibacterial activity

The well diffusion technique was employed to study the antibacterial properties of the chitosan-NiO-amygdalin HNMs. These pathogens, including *Streptococcus pyrogens, Escherichia coli, Bacillus subtilis, Klebesiella pneumonia, Klebesiella terrigena*, and *Klebesiella planticola*, were loaded onto the MHA medium, and wells were created on the surface. The Chitosan-NiO-Amygdalin HNMs samples at various dosages (20, 40, 60, 80, and 100 µg/ml) were then loaded onto the wells, and incubated for 24 h. Following the incubation, the findings were assessed, and the inhibition zones were tabulated.

In vitro assays

Cell collection and maintenance

The liver cancer (Hep3B) and breast cancer (MCF-7) cells were purchased from ATCC, USA. Subsequently, the cells were cultivated on DMEM medium with 10% FBS in a CO_2 incubator at 37°C. After cells reached 80% confluency, they were trypsinized and utilized for further assays.

MTT assay

The MTT assay was done to analyze the cytotoxicity of the Chitosan-NiO-Amygdalin HNMs on Hep3B and MCF-7 cells. Both cells were loaded separately on the 96-well plate and incubated for 24 h. Later, cells were exposed to diverse dosages (1, 2.5, 5, 10, 20, 40, and 60 µg/ml) of the Chitosan-NiO-Amygdalin HNMs for 24, 48, and 72 h time periods. After the treatment, 20µl of MTT reagent and 100µl of DMEM were mixed to the well for 4 h. Subsequently, DMSO (100µl) was mixed to each well in liquefy the formed formazan crystals, and the absorbance was taken at 570nm.

Statistical analysis

The GraphPad Prism Software was utilized for the statistical analyses, and the values are illustrated as the mean±SD of triplicate assays (n = 3). The values are analyzed by the one-way ANOVA and Tukey's *post hoc* assay, and $p<0.05$ was set as significant.

RESULTS

Characterization of the Chitosan-NiO-Amygdalin HNMs

The synthesis of chitosan-NiO-amygdalin HNMs was confirmed by UV-vis spectrophotometry analysis. The absorbance was taken at 200 to 1000 nm. Previous reported that the absorbance edge peak of NiO nanoparticles (NPs) was observed at 330 nm.[16] The combination of Chitosan-NiO-Amygdalin hybrid nanomaterials (HNMs) exhibits absorbance peaks at 311 nm. This shift to a lower wavelength is due to the coating effects of chitosan and amygdalin. (Figure 1A). The PL spectrum of the synthesized Chitosan-NiO-Amygdalin HNMs is presented in Figure 1B.

The emission spectrum of the Chitosan-NiO-Amygdalin HNMs exhibits peaks at 368 nm, 390 nm, 399 nm, 414 nm, 436 nm, 466 nm, 483 nm, and 522 nm, respectively. The UV emissions (near the band edge) are observed at 368 nm, 390 nm, and 399 nm, corresponding to the radiative recombination in the free exciton-exciton collision. The violet emissions at 414 nm and 436 nm are attributed to surface state emissions from recombining trapped electron-hole pairs from dangling bonds in the Chitosan-NiO-Amygdalin HNMs. The violet emissions observed at 414 nm and 436 nm can be attributed to electron transitions from the surface donor level of the nickel interstitials (Ni_i) to the top level of the valence band. The blue emission bands at 466 and 483 nm are associated with singly ionized Ni vacancies (Ni_v). Finally, the green emission band centered at 522 nm is due to oxygen vacancies (Ov).

The XRD patterns of the synthesized Chitosan-NiO-Amygdalin HNMs are presented in Figure 2A. These patterns reveal that the Chitosan-NiO-Amygdalin HNMs possess a cubic crystal structure, with distinct peaks observed at 2θ values of 37.25°, 43.28°, 62.81°, 75.42°, and 79.30°. These peak positions correspond to the (111), (200), (220), (311), and (222) planes of the NiO structure, respectively, in agreement with the data provided by the Joint Committee on Powder Diffraction Standards (JCPDS Card No: 04-0850). Therefore, we can confidently ascertain the highly crystalline nature of the synthesized Chitosan-NiO-Amygdalin HNMs. Additionally, distinct peaks at 20.30° and 12.68° were observed in the XRD pattern, corresponding to chitosan and amygdalin. These peaks suggest the coexistence of chitosan and amygdalin within the NiO matrix, indicating the formation of a hybrid nanostructure. The construction of

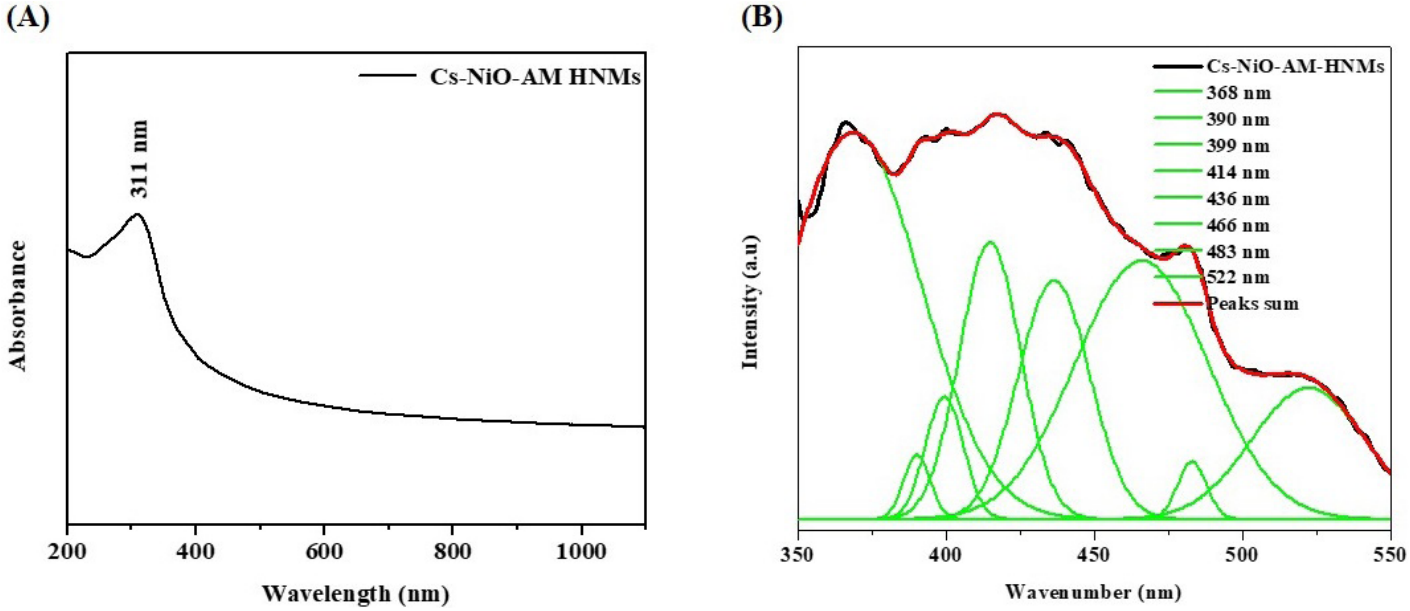

Figure 1: UV-visible spectroscopy and photoluminescence (PL) analysis of the Chitosan-NiO-Amygdalin HNMs. A): The absorbance of the sample was measured at 200 to 1000 nm, demonstrating a maximum absorbance peak at 311 nm, which evidences the presence of Chitosan-NiO-Amygdalin HNMs. B): The PL emission spectrum of the synthesized Chitosan-NiO-Amygdalin HNMs exhibits various peaks at 368, 390, 399, 414, 436, 466, 483, and 522 nm, respectively, which proves the optoelectronic properties.

this hybrid nanostructure can be attributed to steric effects and intermolecular hydrogen bonding interactions among chitosan, NiO, and amygdalin. The crystallite size D was used to calculate the Debye-Scherrer relation. Average crystallite size D = The average crystallite size of the Chitosan-NiO-Amygdalin HNMs, calculated at 35 nm. The DLS analysis was done to assess the hydrodynamic size of the prepared Chitosan-NiO-Amygdalin HNMs, as shown in Figure 2B. The study reveals reasonably small agglomeration with an average hydrodynamic diameter of 43.90 nm. Furthermore, the DLS particle size was consistent with the XRD and TEM findings.

The morphology of the Chitosan-NiO-Amygdalin HNMs was analyzed through FESEM analysis, as shown in Figure 3. At lower (Figure 3a) and higher magnifications (Figure 3b), the images reveal that the Chitosan-NiO-Amygdalin HNMs exhibit hexagonal structures with some degree of aggregation, typical of hybrid material formation. The average particle sizes of the Chitosan-NiO-Amygdalin HNMs are the range of 50-60 nm. These observations confirm the successful coating of chitosan and amygdalin with the NiO surface matrix. These interactions can be attributed to the electrostatic forces between the chitosan-NiO-amygdalin surface matrix components. An EDAX spectrum of the Chitosan-NiO-Amygdalin HNMs is presented in Figure (3c). The major elements identified were nickel (Ni) at 45.59%, oxygen (O) at 43.70%, carbon (C) at 8.34%, and nitrogen (N) at 2.36%, confirming their presence in the chitosan-NiO-amygdalin HNM nanocomposite. The EDAX analysis provides further confirmation of the formation of the Chitosan-NiO-Amygdalin HNMs.

TEM images and SAED patterns of Chitosan-NiO-Amygdalin HNMs. Figure 4 (a-e) illustrates the synthesis of Chitosan-NiO-Amygdalin HNMs, which exhibit a hexagonal morphology and possess an average size of 40 nm. During the formation of the Chitosan-NiO-Amygdalin HNMs, significant aggregation was occurred. This phenomenon is attributed to the high surface-area-to-volume ratio of the nanomaterial, resulting in very high surface energy. The nanomaterial's surface energy is reduced, leading to aggregation onto the nanomaterial surface matrix. The crystallization of the Chitosan-NiO-Amygdalin HNMs was confirmed by the SAED patterns (Figure 4f).

The FT-IR spectra reveal the functional groups of the biomolecules (chitosan, amygdalin) with NiO HNMs Figure 5. The FT-IR spectra of the biomolecule chitosan reveals the hydrogen (-OH) bond, and the amide (-NH) I group is observed at 3432 cm^{-1} and 1662 cm^{-1}, respectively. The carboxylic acid (COO^-) peaks at 1377 cm^{-1} and 1042 cm^{-1} correspond to the glucose circle for stretching C-O-C. The functional characteristics of amygdalin include asymmetric and symmetric peaks detected at 2928 cm^{-1} and 2878 cm^{-1}, respectively, due to the C-H group. The C-O stretching peak is 1115 cm^{-1}, and the HCCH out-of-plane bending peak is 943 cm^{-1}. The figure illustrates the distinct functional groups of chitosan, amygdalin, and NiO in HNMs. Chitosan characteristics peaks were found at 3631 and 3425 cm^{-1} wavenumbers for O-H and N-H with hydrogen bonds. Amygdalin peaks include asymmetric and symmetric (C-H) peaks at 2923 cm^{-1} and 2852 cm^{-1}, respectively. The acetyl CO stretching peaks were noted at 1648 cm-1 and 1050 cm^{-1}, respectively. The CH3 symmetrical angular deformation peak was observed at 1399 cm^{-1}. The metal-oxide (Ni-O) stretching band modes were noted at 694, 567, and 452 cm^{-1}, respectively. The hybrid formation of

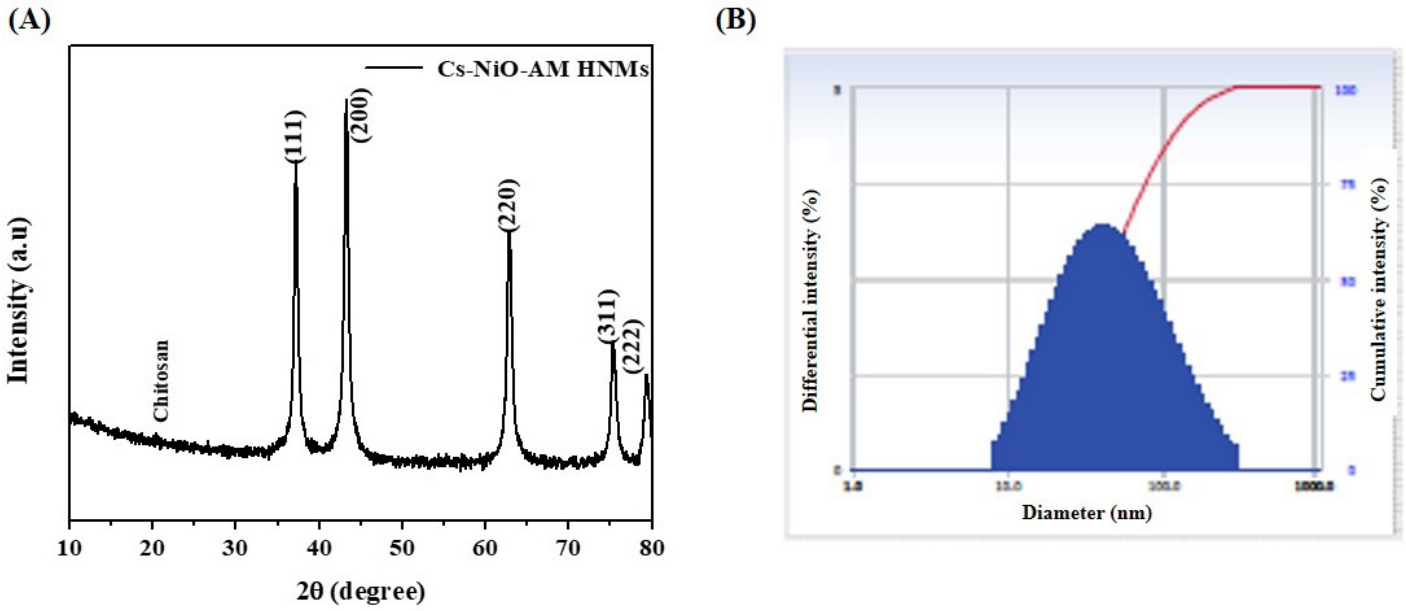

Figure 2: XRD and DLS analyses of the Chitosan-NiO-Amygdalin HNMs. A): The XRD patterns of the synthesized Chitosan-NiO-Amygdalin HNMs possess a cubic crystal structure with a crystalline nature. B): The DLS analysis revealed the agglomeration of particles with an average hydrodynamic diameter of 43.90 nm.

Chitosan-NiO-Amygdalin HNMs confirms these peaks due to the intermolecular hydrogen bonds between the biopolymer (chitosan), organic (amygdalin), and inorganic (NiO) surface matrix (Figure 5).

Antibacterial effects of the Chitosan-NiO-Amygdalin HNMs

The antibacterial properties of Chitosan-NiO-Amygdalin HNMs against various pathogens, such as *S. pyrogens, E. coli, B. subtilis, K. pneumonia, K. terrigena*, and *K. planticola*, were analyzed using the well diffusion technique (Table 1). The treatment of HNMs with different concentrations demonstrated significant antibacterial effectiveness against all tested pathogens. The growth of several strains, specifically *E. coli, B. subtilis*, and*K. planticola*, was successfully inhibited by Chitosan-NiO-Amygdalin HNMs. The minimum inhibitory concentrations of the Chitosan-NiO-Amygdalin HNMs are depicted in Table 2.

Cytotoxic effects of the Chitosan-NiO-Amygdalin HNMs

An MTT cytotoxic assay was done to assess the cytotoxic properties of the Chitosan-NiO-Amygdalin HNMs on both MCF-7 and HepB3 cells at 24, 48, and 72 h time intervals. The findings are illustrated in Figure 6(A and B). The findings demonstrate that the treatment of Chitosan-NiO-Amygdalin HNMs at diverse dosages (1, 2.5, 5, 10, 20, 40, and 60 µg/ml) remarkably diminished the viability of both MCF-7 and Hep3B cells. Both cell viability exhibited a significant decline at increasing concentrations of Chitosan-NiO-Amygdalin HNMs compared to untreated cells. However, the MCF-7 cells showed more sensitivity to the Chitosan-NiO-Amygdalin HNMs treatment than the Hep3B cells, as shown by the assay results.

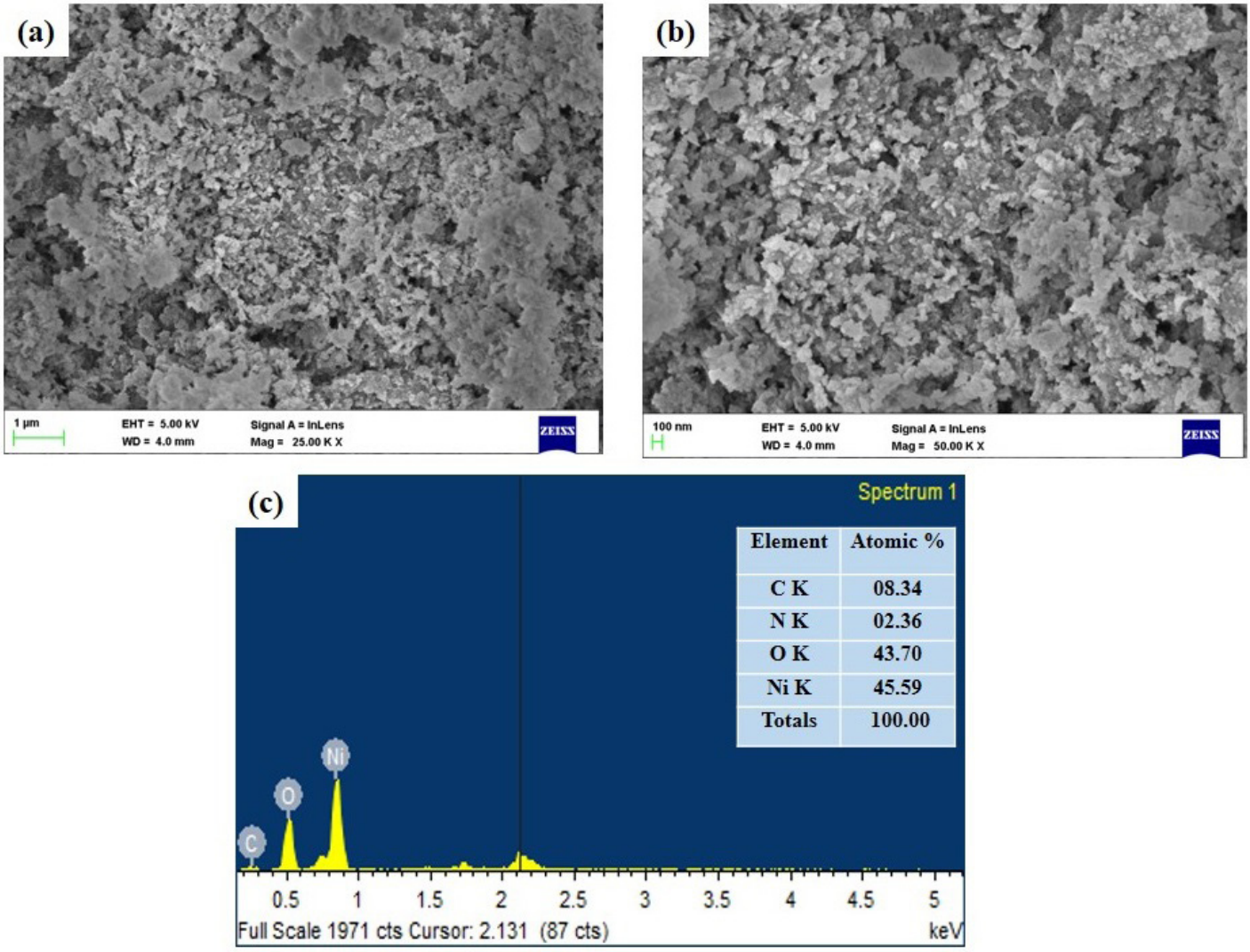

Figure 3: FE-SEM and EDX analyses of the Chitosan-NiO-Amygdalin HNMs. a): The lower and b): higher magnification images of the Chitosan-NiO-Amygdalin HNMs exhibit hexagonal structures with some degree of aggregation, typical of hybrid material formation with an average particle size of 50-60 nm. c): An EDAX spectrum of the Chitosan-NiO-Amygdalin HNMs showed the presence of major elements identified: nickel (Ni) at 45.59%, oxygen (O) at 43.70%, carbon (C) at 8.34%, and nitrogen (N) at 2.36%, confirming their presence in the HNMs.

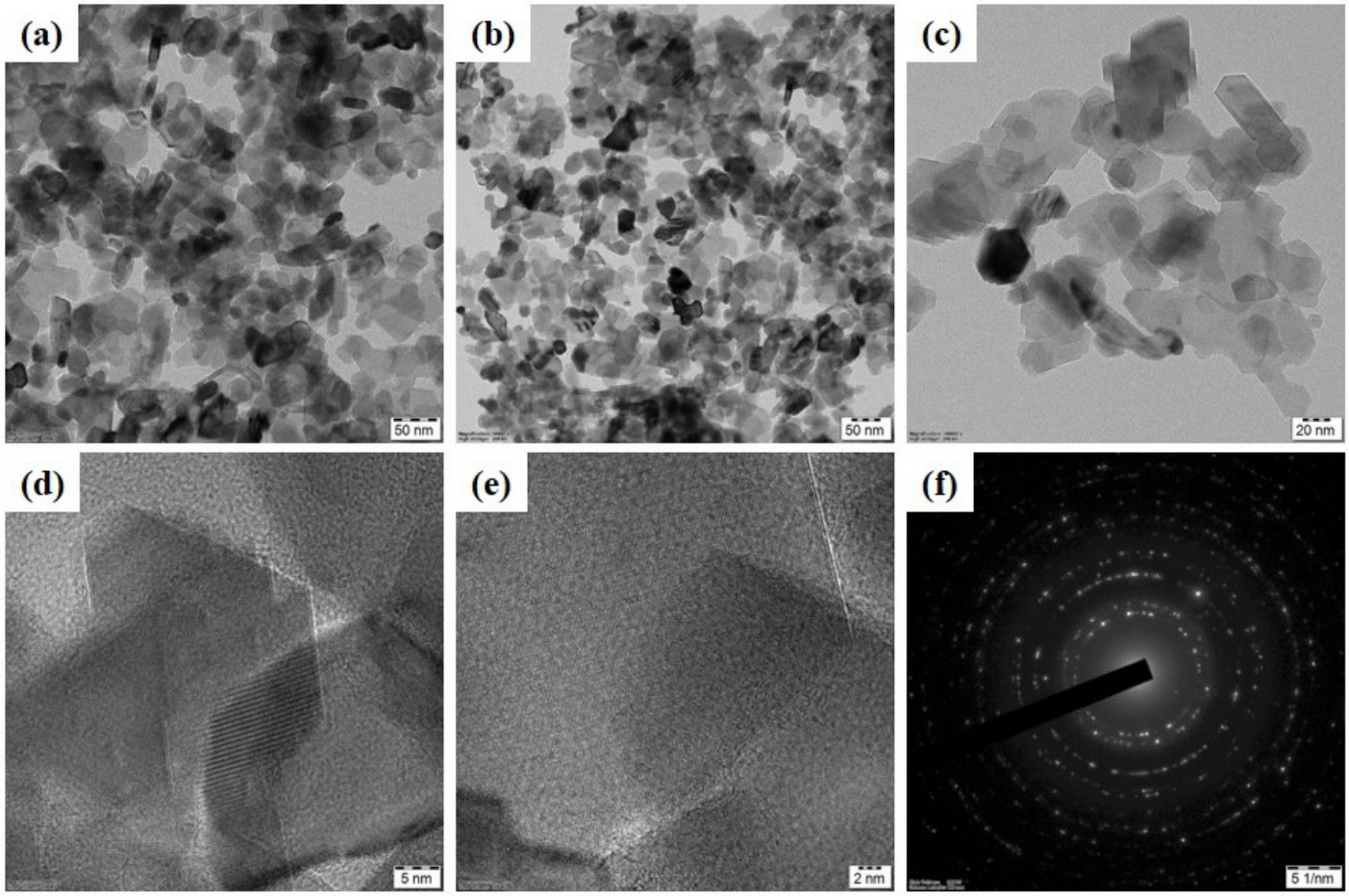

Figure 4: TEM and SAED pattern of the Chitosan-NiO-Amygdalin HNMs. a-e): The TEM images illustrate the formation of Chitosan-NiO-Amygdalin HNMs with hexagonal morphology and an average size of 40 nm. f): The SAED patterns confirmed the crystallization of the Chitosan-NiO-Amygdalin HNMs.

Table 1: Antibacterial effects of the Chitosan-NiO-Amygdalin HNMs.

Sl. No	Bacterial Strain	Concentration of the sample (µg/ml) Zone of inhibition (mm)				
Gram Positive		20 µg	40 µg	60 µg	80 µg	100 µg
1	A-*Streptococcus pyrogens*	7	9	12	15	21
2	B-*E. coli*	6	8	11	16	22
3	C-*Bacillus subtilis*	8	9	12	18	23
Gram negative						
1	A-*Klebesiella pneumonia*	8	10	11	15	20.5
2	B-*Klebesiella terrigena*	9	11	12	16	21
3	C-*Klebesiella planticola*	10	12	14	18	22.3

DISCUSSION

In recent decades, there has been substantial research on various inorganic nanoparticles because of their wide range of practical applications in several domains, like biomedicine.[17] NiO nanoparticles have the distinct advantages of being cost-effective, non-toxic, and exhibiting exceptional stability as conductive materials. These nanoparticles were also employed for various medical purposes, such as imaging, drug distribution, biological detection, and antibiotics.[18,19] Chitosan nanoparticles enable the controlled release of drugs through the breakdown of chitosan. The hydrophobic properties of chitosan and the self-assembly of nanoparticles in a fluid arrangement allow for effective adsorption of hydrophobic medicines and their controlled release. Consequently, it has the ability to serve as an outstanding carrier for drugs.[20,21] Chitosan nanoparticles were discovered to possess an extended duration of circulation, hence aiding in the prevention of adhesion. Additionally, these nanoparticles demonstrated selectivity for cancer cells, displaying sensitivity to changes in pH.[22]

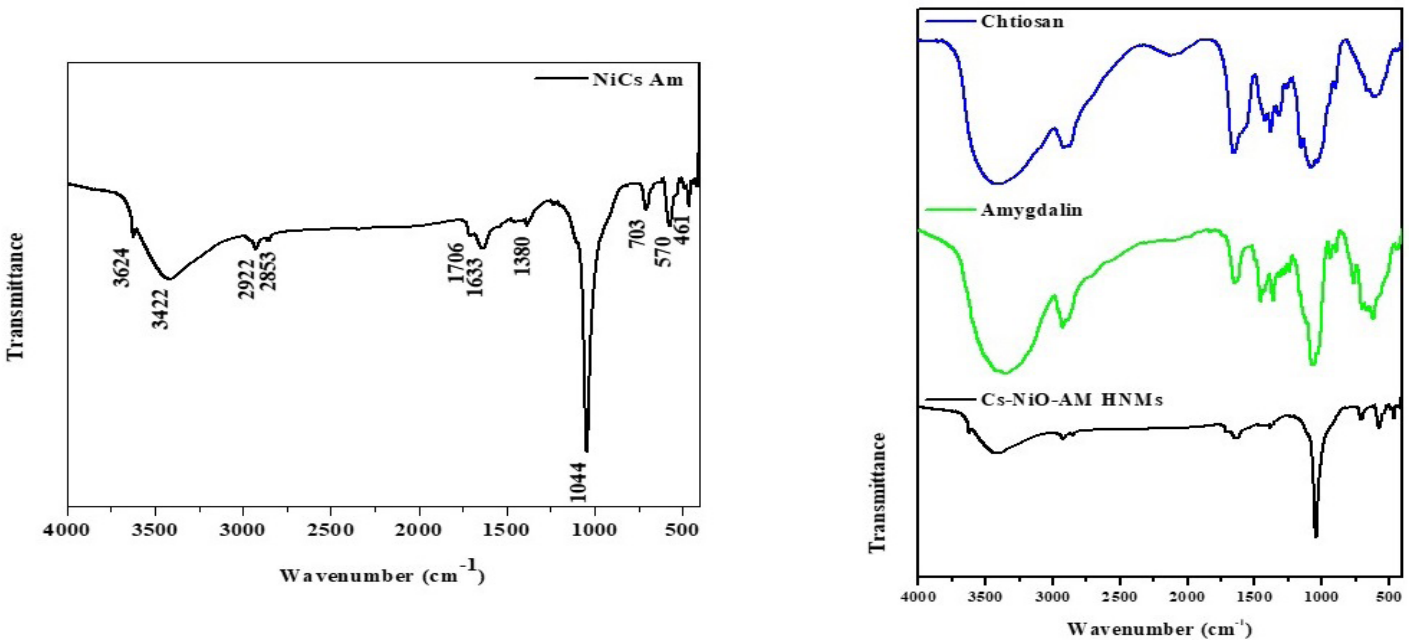

Figure 5: FT-IR analysis of the Chitosan-NiO-Amygdalin HNMs. The FT-IR spectra of the Chitosan-NiO-Amygdalin HNMs exhibited absorption peaks at various wave numbers, indicating the presence of many functional groups.

Table 2: Minimum inhibitory concentrations of the Chitosan-NiO-Amygdalin HNMs.

Sl. No	Bacterial Strain	MIC (µg/ml)	MBC(µg/ml)
1	A-*Streptococcus pyrogens*	50±0.58	6.58±0.65
2	B-*E. coli*	12.5±1.2	8.53±0.78
3	C-*Bacillus subtilis*	15.6±0.69	9.65±0.89
Gram negative			
1	A-*Klebesiella pneumonia*	18.9±0.94	10.23±0.95
2	B-*Klebesiella terrigena*	15.2±0.62	9.85±1.23
3	C-*Klebesiella planticola*	17.5±0.61	10.2±0.98

The values are statistically analyzed by one-way ANOVA and Tukey's post hoc assay using the GraphPad Prism software. The data are not sharing common superscript and significantly vary at $p<0.05$ from untreated control.

In this study, the Chitosan-NiO-Amygdalin HNMs were formulated and characterized using numerous methods. The synthesis of Chitosan-NiO-Amygdalin HNMs was confirmed by a UV-vis spectrophotometry study. The emission spectrum of the Chitosan-NiO-Amygdalin HNMs in PL analysis exhibits various peaks, which show their optoelectronic properties. The XRD patterns reveal that the Chitosan-NiO-Amygdalin HNMs possess a cubic crystal structure. The DLS analysis was done to measure the hydrodynamic size of the prepared Chitosan-NiO-Amygdalin HNMs, and the results showed a small agglomeration with an average hydrodynamic diameter of 43.90 nm, which is consistent with the XRD and TEM findings. The SEM images revealed that the Chitosan-NiO-Amygdalin HNMs exhibit hexagonal structures with aggregated form. An EDAX spectrum showed the presence of major elements identified as Ni, O, C, and N. The EDAX analysis provides further confirmation of the formation of the HNMs. TEM is the most effective technique for accurately identifying the size and morphological characteristics of a nanostructure. TEM images illustrate the synthesis of Chitosan-NiO-Amygdalin HNMs with hexagonal morphology and an average size of 40 nm. The FT-IR analysis was done to study the functional groups responsible for reducing, capping, and stabilizing the produced nanoparticles. The FT-IR spectra of HNMs exhibited various absorption peaks, indicating the occurrence of many functional groups.

Cancer is a pathological condition characterized by the abnormal proliferation and spreading of a group of cells within the body. Various factors influence the development of cancer, such as toxin exposure, alcohol, infections, and the existence of metabolic disorders.[23] Human cells undergo cell division, a natural and vital process that facilitates the proliferation and growth of normal and healthy cells, resulting in the generation of new cells in the body. Cellular damage, or senescence, results in cell death, prompting the body to regenerate and replace them with new

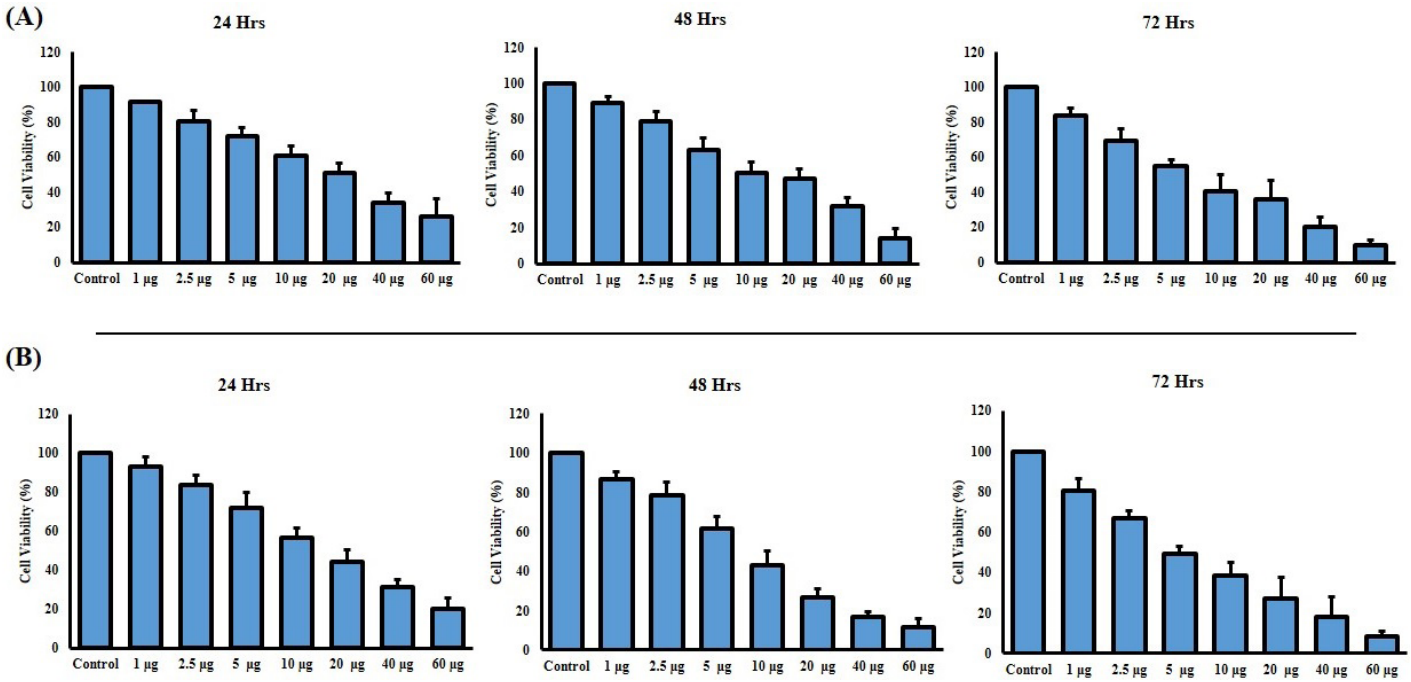

Figure 6: Effect of Chitosan-NiO-Amygdalin HNMs on the viability of (A) liver cancer Hep3B and (B) breast cancer MCF-7 cells. The results demonstrate that the treatment of HNMs at different concentrations of significantly inhibited the viability of both MCF-7 and Hep3B cells at 24, 48, and 72 h time periods. The values are depicted as a mean±SD of triplicate measurements (n = 3). The values are statistically analyzed by one-way ANOVA and Tukey's post hoc assay using the GraphPad Prism software.

cells.[24] Occasionally, this interruption results in the development and spread of anomalous cells (cancerous cells). In cancer, the uncontrolled growth and spread of somatic cells leads to the destruction of healthy tissues through destabilization, erosion, and invasion.[25]

Multidrug resistance (MDR) in pathogenic bacteria is a universal public health issue since the treatment of bacterial infections that are resistant to several drugs using current antibiotics becomes increasingly difficult.[26] The increase of MDR pathogenic microorganisms poses a significant issue for global public health. MDR bacteria pose several health risks, including the spread of infectious diseases and the potential to hinder the success of important medical treatments such as surgery, organ transplantation, and cancer treatment.[27] There are many cases of infections due to the MDR bacteria, which can be extremely difficult to treat and cause significant death rates worldwide.[28] As per the World Health Organization, drug-resistant diseases are currently causing the deaths of at least 700,000 cases annually.[29] The MDR bacteria encompass a range of species, such as *K. pneumoniae, S. pneumoniae, E. coli*, etc.[30] Gradually, a growing number of bacteria are developing resistance to antibiotics. Hence, there is an immense need to develop innovative, safe, and efficient antibacterial candidates to manage MDR infections. In the present study, the synthesized Chitosan-NiO-Amygdalin HNMs showed significant antibacterial properties against the tested strains. More specifically, *E. coli, B. subtilis*, and*K. planticola* showed more sensitivity to the chitosan-NiO-amygdalin HNMs.

Chitosan-NiO-Amygdalin hybrid nanomaterials (HNMs) show significant potential in combating multidrug-resistant (MDR) bacteria by employing a multifaceted approach that differs from traditional antibiotics. While current antibiotics target specific bacterial processes, which MDR strains often evade through resistance mechanisms, these HNMs combine the antibacterial properties of chitosan, which disrupts bacterial cell membranes, with the oxidative stress induced by NiO nanoparticles and the metabolic interference from amygdalin. This synergistic effect not only enhances antibacterial activity but also reduces the likelihood of resistance development. Moreover, the biocompatibility and safety of these HNMs, due to the natural and non-toxic nature of chitosan and the controlled use of NiO and amygdalin, make them a promising alternative to traditional antibiotics, potentially overcoming the challenges posed by MDR bacteria.

Nanoparticle-mediated drug delivery systems have the potential to increase the bioavailability and antitumor efficacy of chemotherapeutic drugs.[31] Furthermore, these formulations have the potential to alter the biodistribution of the drugs in the body, decrease the development of drug resistance, lower non-specific toxicity, and protect the drugs from enzymatic breakdown.[32,33] Nanocarriers provide more specificity in delivering drugs to specified targets by using both active and passive targeting mechanisms.[34] Nanoparticle-mediated targeted drug delivery provides several benefits over traditional chemotherapy for cancer treatment. These benefits include reduced toxicity in healthy cells, prevention of drug degradation, and improved specificity.[35] In this study, the effect of Chitosan-NiO-Amygdalin HNMs on the

growth of both Hep3B and MCF-7 cells was assessed at different time periods. The results demonstrated that the synthesized Chitosan-NiO-Amygdalin HNMs at various concentrations effectively reduced the growth of both MCF-7 and Hep3B cells. These results showed the cytotoxic effects of chitosan-NiO-amygdalin HNMs against both liver and breast cancer cells.

CONCLUSION

The present study has found that synthesized Chitosan-NiO-Amygdalin HNMs have a significant effect on inhibiting the viability of both Hep3B and MCF-7 cells. The Chitosan-NiO-Amygdalin HNMs have also shown potential antibacterial effects against various pathogens. Hence, the findings suggest that Chitosan-NiO-Amygdalin HNMs exhibit potential to be a prospective therapeutic agent in the future. Nevertheless, further extensive analyses are still required to fully comprehend the various therapeutic roles of the Chitosan-NiO-Amygdalin HNMs against cancer and other diseases.

ACKNOWLEDGEMENT

This project was supported by Researchers Supporting Project number (RSP2024R177) King Saud University, Riyadh, Saudi Arabia.

CONFLICT OF INTEREST

The authors declare no conflict of interest.

ABBREVIATIONS

Hep3B: liver cancer; **MCF-7:** Breast cancer; **PL:** Photoluminescence; **XRD:** X-ray diffraction; **DLS:** Dynamic light scattering; **SEM:** Scanning electron microscopy; **TEM:** Transmission electron microscopy; **FT-IR:** Fourier transform infrared; **NiO:** Nickel oxide; **HNMs**: Hybrid nanomaterials; **MHA:** Muller-Hinton agar; **DMEM:** Dulbecco's modified Eagle's medium; **FBS:** Fetal bovine serum; ***S. pyrogens*:** *Streptococcus pyrogens;* ***E. coli*:** *Escherichia coli*; ***B. subtilis*:** *Bacillus subtilis*; ***K. pneumonia*:** *Klebesiella pneumonia*; ***K. terrigena*:** *Klebesiella terrigena*; ***K. planticola*:** *Klebesiella planticola*.

SUMMARY

The study results of the various characterization analyses showed the formation of metallic Chitosan-NiO-Amygdalin HNMs. The treatment of Chitosan-NiO-Amygdalin HNMs significantly decreased cell viability, and potential antibacterial effects against various pathogens. Hence, the present findings indicate that Chitosan-NiO-Amygdalin HNMs hold potential as a highly effective candidate for reduced the growth of both MCF-7 and Hep3B cells. These results showed the cytotoxic effects of chitosan-NiO-amygdalin HNMs against both liver and breast cancer cells.

REFERENCES

1. Doroudian M, Zanganeh S, Abbasgholinejad E, Donnelly SC. Nanomedicine in Lung Cancer Immunotherapy. Front Bioeng Biotechnol. 2023;11:1144653.
2. Barbero F, Gul S, Perrone G, Fenoglio I. Photoresponsive Inorganic Nanomaterials in Oncology. Technol Cancer Res Treat. 2023;22:15330338231192850.
3. Nasir A, Khan A, Li J, Naeem M, Khalil AAK, Khan K, Qasim M. Nanotechnology, A Tool for Diagnostics and Treatment of Cancer. Curr Top Med Chem. 2021;21(15):1360-1376.
4. Veselov VV, Nosyrev AE, Jicsinszky L, Alyautdin RN, Cravotto G. Targeted Delivery Methods for Anticancer Drugs. Cancers (Basel). 2022;14(3):622.
5. Boros BV, Dascalu D, Ostafe V, Isvoran A. Assessment of the Effects of Chitosan, Chitooligosaccharides and Their Derivatives on Lemna Minor. Molecules. 2022;27:6123.
6. Muxika A, Etxabide A, Uranga J, Guerrero P, de la Caba K. Chitosan as a Bioactive Polymer: Processing, Properties and Applications. Int. J. Biol. Macromol. 2017;105:1358-1368.
7. Ukoba K, Eloka-Eboka A, Inambao F. Review of nanostructured NiO thin film deposition using the spray pyrolysis technique. Renew Sust Energ Rev. 2018;82:2900-2915.
8. Siegel RL, Miller KD, Fuchs HE, Jemal A. Cancer statistics 2021. CA Cancer J. Clin. 2021;71:7-33.
9. Sung HA, Ferlay J, Siegel RL, Laversanne M, Soerjomataram I, Jemal A, Bray F. Global cancer statistics 2020: GLOBOCAN estimates of incidence and mortality worldwide for 36 cancers in 185 countries. CA Cancer J. Clin. 2021;71:209-449.
10. Fulton MD, Najahi-Missaoui W. Liposomes in Cancer Therapy: How Did We Start and Where Are We Now. Int J Mol Sci. 2023;24(7):6615.
11. Kim JY, Hong HL, Kim GM, Leem J, Kwon HH. Protective Effects of Carnosic Acid on Lipopolysaccharide-Induced Acute Kidney Injury in Mice. Molecules. 2021;26:7589.
12. Makarevic J, Rutz J, Juengel E, Kaulfuss S, Reiter M, Tsaur I, et al. Amygdalin blocks bladder cancer cell growth *in vitro* by diminishing cyclin A and cdk2. PLoS One. 2014;9 (8):e105590.
13. Lee HM, Moon A. Amygdalin regulates apoptosis and adhesion in Hs578T triple-negative breast cancer cells. Biomol. Ther. 2016;24 (1):62-66.
14. Saleem M, Asif J, Asif M, Saleem U. Amygdalin from apricot kernels induces apoptosis and causes cell cycle arrest in cancer cells: An updated review. Anticancer. Agents Med. Chem. 218;18 (12):1650-1655.
15. Christodoulou P, Boutsikos P, Neophytou CM, Kyriakou TC, Christodoulou MI, Papageorgis P, Stephanou A, Patrikios I. Amygdalin as a chemoprotective agent in co-treatment with cisplatin. Front Pharmacol. 2022;13:1013692.
16. El-Kemary M, Nagy N, El-Mehasseb I. Nickel oxide nanoparticles: synthesis and spectral studies of interactions with glucose. Materials Science in Semiconductor Processing. 2013;16(6):1747-52.
17. Gebreslassie YT, Gebretnsae HG. Green and cost-effective synthesis of tin oxide nanoparticles: a review on the synthesis methodologies, mechanism of formation, and their potential applications. Nanoscale Res Lett. 2021;16(1):97.
18. Jaji ND, Lee HL, Hussin MH, Akil HM, Zakaria MR, Othman MBH. Advanced nickel nanoparticles technology: from synthesis to applications. Nanotechnol Rev. 2020;9(1):1456-1480.
19. Brigger I, Dubernet C, Couvreur P. Nanoparticles in cancer therapy and diagnosis. Adv Drug Deliv Rev. 2012;64:24-36.
20. Tang W, Wang J, Hou H, Li Y, Wang J, Fu J, Lu L, Gao D, Liu Z, Zhao F, et al. Review: Application of chitosan and its derivatives in medical materials. Int. J. Biol. Macromol. 2023;240:124398.
21. Tavakoli M, Labbaf S, Mirhaj M, Salehi S, Seifalian AM, Firuzeh M. Natural polymers in wound healing: From academic studies to commercial products. J. Appl. Polym. Sci. 2023;140:e53910.
22. Motiei M, Kashanian S, Lucia LA, Khazaei M. Intrinsic parameters for the synthesis and tuned properties of amphiphilic chitosan drug delivery nanocarriers. J. Control. Release. 2017;260:213-225.
23. Ogunwobi OO, Harricharran T, Huaman J, Galuza A, Odumuwagun O, Tan Y, Ma GX, Nguyen MT. Mechanisms of Hepatocellular Carcinoma Progression. World J. Gastroenterol. 2019;25:2279-2293.
24. Sachdeva P, Ghosh S, Ghosh S, Han S, Banerjee J, Bhaskar R, Sinha JK. Childhood Obesity: A Potential Key Factor in the Development of Glioblastoma Multiforme. Life. 2022;12:1673.
25. Koo MM, Swann R, McPhail S, Abel GA, Elliss-Brookes L, Rubin GP, Lyratzopoulos G. Presenting Symptoms of Cancer and Stage at Diagnosis: Evidence from a Cross-Sectional, Population-Based Study. Lancet Oncol. 2020;21:73-79.
26. van Duin D, Paterson DL. Multidrug-Resistant Bacteria in the Community: Trends and Lessons Learned. Infect. Dis. Clin. N. Am. 2016;30:77-390.
27. Perez F, van-Duin D. Carbapenem-resistant Enterobacteriaceae: A menace to our most vulnerable patients. Clevel. Clin. J. Med. 2013;80:225-233.
28. Ferri M, Ranucci E, Romagnoli P, Giaccone V. Antimicrobial resistance: A global emerging threat to public health systems. Crit. Rev. Food Sci. 2017;57:2857-2876.
29. World Health Organization . Global Action Plan on Antimicrobial Resistance. World Health Organization; Geneva, Switzerland. 2017;1-28.
30. Neut C. Carriage of Multidrug-Resistant Bacteria in Healthy People: Recognition of Several Risk Groups. Antibiotics. 2021;10:1163.

31. Yan L, Shen J, Wang J, Yang X, Dong S, Lu S. Nanoparticle-Based Drug Delivery System: A Patient-Friendly Chemotherapy for Oncology: A publication of International Hormesis Society. Dose Response. 2020;18:1559325820936161.
32. Rana V, Sharma R. Chapter 5-Recent Advances in Development of Nano Drug Delivery. In: Mohapatra S.S., Ranjan S., Dasgupta N., Mishra R.K., Thomas S., editors. Applications of Targeted Nano Drugs and Delivery Systems. Elsevier; Amsterdam, The Netherlands: 2019;93-131.
33. Lu H, Zhang S, Wang J, Chen Q. A Review on Polymer and Lipid-Based Nanocarriers and Its Application to Nano-Pharmaceutical and Food-Based Systems. Front. Nutr. 2021;8:783831.
34. Harun NA, Benning MJ, Horrocks BR, Fulton DA. Gold nanoparticle-enhanced luminescence of silicon quantum dots co-encapsulated in polymer nanoparticles. Nanoscale. 2013;5:3817-3827.
35. Zhang H, Lv J, Jia Z. Efficient Fluorescence Resonance Energy Transfer between Quantum Dots and Gold Nanoparticles Based on Porous Silicon Photonic Crystal for DNA Detection. Sensors (Basel) 2017;17.

Cite this article: Saravanan K, Bharathi M, Alyami NM, Alharbi SA, Ali SHHA, Arulselvan P. Synthesis and Characterization of Novel Chitosan-Nickel oxide Based Amygdalin Hybrid Nanomaterials for Antibacterial and Anticancer Properties. Indian J of Pharmaceutical Education and Research. 2024;58(4):1225-34.